Bull. Mater. Sci., Vol. 34, No. 6, October 2011, pp. 1163–1171. © Indian Academy of Sciences.

Nanocrystalline TiO_2 preparation by microwave route and nature of anatase–rutile phase transition in nano TiO_2

G M NEELGUND[†], S A SHIVASHANKAR[†], B K CHETHANA, P P SAHOO and K J RAO[*]
Solid State and Structural Chemistry Unit, [†]Materials Research Centre, Indian Institute of Science, Bangalore 560 012, India

MS received 27 July 2011

Abstract. **Nanopowders of TiO_2 has been prepared using a microwave irradiation-assisted route, starting from a metalorganic precursor, *bis*(ethyl-3-oxo-butanoato)oxotitanium (IV), $[TiO(etob)_2]_2$. Polyvinylpyrrolidone (PVP) was used as a capping agent. The as-prepared amorphous powders crystallize into anatase phase, when calcined. At higher calcination temperature, the rutile phase is observed to form in increasing quantities as the calcination temperature is raised. The structural and physicochemical properties were measured using XRD, FT–IR, SEM, TEM and thermal analyses. The mechanisms of formation of nano-TiO_2 from the metal–organic precursor and the irreversible phase transformation of nano TiO_2 from anatase to rutile structure at higher temperatures have been discussed. It is suggested that a unique step of initiation of transformation takes place in $Ti_{1/2}O$ layers in anatase which propagates. This mechanism rationalizes several key observations associated with the anatase–rutile transformation.**

Keywords. **TiO_2; microwave irradiation; anatase; rutile; metalorganic synthesis; PVP.**

1. Introduction

In the recent years, intense effort has been made on the preparation of nanocrystals of metal oxides, as they exhibit markedly different physical and chemical properties compared to their bulk form. In particular, nanocrystalline TiO_2 is one of the most studied oxides, owing to its wide application in photocatalysis, as in self-cleaning glasses (Kominami *et al* 2002; Parking and Palgrave 2005; Ohshima *et al* 2006), in solar energy conversion (Nakade *et al* 2002; Jang *et al* 2006), in the preparation of ductile ceramics (Karch *et al* 1987), in sensors (Zhu *et al* 2002), and in mesoporous membranes (Wei *et al* 2006). Industrially, TiO_2 is perhaps next only to silver and carbon (PEW 2009) in term of the quantities of nanomaterials in use. The technological potential of titania is expected to be remarkably extended if a fine-tuning of particle morphology can be achieved. Nanosized anatase and rutile particles have well known industrial applications (Matsunaga and Inagaki 2006). Rutile is thermodynamically more stable than anatase and is characterized by a smaller bandgap energy of 3 eV than anatase (3·2 eV). Rutile exhibits higher chemical stability, refractive index and tinting strength, lower photoreactivity, and is cheaper to produce. The main application of rutile powders is as white pigment in paints. Nanoparticles of rutile are now used as UV-protective material in cosmetics. Anatase is a metastable phase and is preferred as a heterogeneous photocatalyst in solar cells for the production of hydrogen and also electrical energy. In the form of powder suspension or immobilized thin film (Baldassari *et al* 2005), it is used for decontamination of water.

A variety of preparative methods of TiO_2 have been reported in the literature, each with its characteristic scope and limitations (Cozzoli *et al* 2003; Tang *et al* 2005; Murugan *et al* 2006). The method of preparation and the starting materials seem to bear profound influence on the formation of TiO_2 nanocrystallites and their morphologies. A microwave method of preparation of nanoparticles of TiO_2 is presented here. It is now well established that the microwave method is fast, simple and efficient (Panneerselvam and Rao 2003a; Kumar *et al* 2004; Panda *et al* 2006). It is also a well recognized green chemistry technique. Reaction times are significantly reduced and the reaction mechanisms are generally very different in microwave synthesis (Panneerselvam and Rao 2003b). The microwave method provides the advantage of uniform, rapid and volumetric heating. In microwave synthesis, the growth rate of products is very high for small particle sizes and, nearly always, the product exhibits a narrow particle size distribution as a consequence of fast homogenous nucleation (Jansen *et al* 1992).

This work reports synthesis of titania nanoparticles starting from a metalorganic precursor, using a microwave irradiation technique. It is shown that the irradiation durations required are remarkably short. Various operational parameters have been varied systematically, so that a deeper understanding of the mechanism of nanoparticle formation is

[*]Author for correspondence (kalyajrao@yahoo.co.in)

obtained. The observed phase transformation of TiO_2 from anatase to rutile is also discussed and a new perspective is provided to rationalize the transition behaviour, by giving due recognition to the presence of distorted close packing of oxygen ions in both anatase and rutile structures. It is also suggested that the presently used microwave method of preparing oxide nanoparticles starting with metalorganic precursors can be a generic approach.

2. Experimental

The metalorganic precursor used for the preparation of nanophase TiO_2 is a oxo-β-ketoesterate complex, viz. *bis*(ethyl-3-oxo-butanoato)oxotitanium (IV), $[TiO(etob)_2]_2$. The precursor was synthesized by a method similar to the one reported earlier (Shalini *et al* 2005) in the literature and its molecular structure is given below.

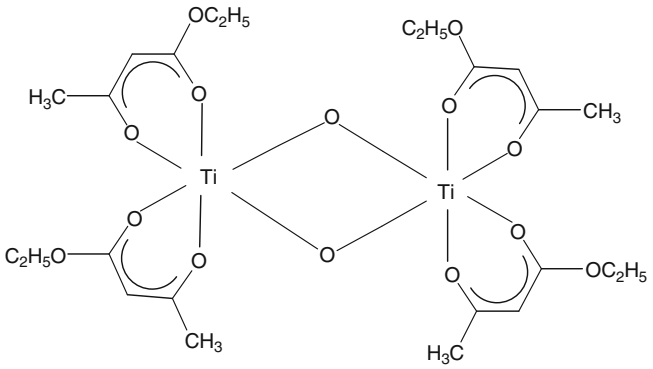

In our laboratory preparation of TiO_2, 5 g of $[TiO(etob)_2]_2$ was dissolved in 100 ml of ethylacetate, 0·2 g of polyvinylpyrrolidone (PVP) was added to the solution as a capping agent, and stirred for 30 min. This resulted in a homogeneous solution which was kept in a round bottomed flask fitted with a water-cooled refluxing system. A domestic (LG Scientific MS283MC 800 W) microwave oven operating at 2·45 GHz with a six-stage variable power was slightly modified to accommodate the round-bottomed flask with the attached refluxing system. The refluxing condenser was made to project out vertically from the top of the oven. The microwave power level was adjusted such that the contents did not boil violently. The oven was kept switched on for just 10 min for irradiation, the contents were allowed to cool, transferred to centrifugation tubes, centrifuged for 10 min and the fine deposits at the bottom of the tubes were recovered after decanting the supernatant liquid. The precipitate was repeatedly washed with acetone and recentrifuged. The wet samples were dried at room temperature and heated for a few min in air at ~500°C to get rid of the capping agent. Titania powder derived from the microwave irradiation technique was calcined at temperatures up to 800°C to study their phase stability and microstructural evolution.

The solid samples were characterized using powder X-ray diffraction (XRD) (Phillips Expert® diffractometer with CuK_α radiation). Fourier-transform infrared (FT–IR) spectra were obtained using a JASCO, FT–IR-610 FT–IR spectrometer with a resolution of 4 cm^{-1} (KBr was used as a reference). Morphologies and particle sizes of selected samples were determined with scanning electron microscopy (JEOL, JSM-5600 LV) and transmission electron microscopy (Philips 420). The as-synthesized TiO_2 was subjected to thermogravimetric analysis (Perkin-Elmer-Pyris Diamond) to determine the possible decomposition and phase transition.

3. Results and discussion

We first discuss the possible mechanisms responsible for formation of TiO_2 under microwave irradiation. It appears that there are two mechanisms, which lead to TiO_2 formation. For convenience, we represent $[TiO(etob)_2]_2$ as $[TiOR_2]_2$, where R is the organic part of the precursor,

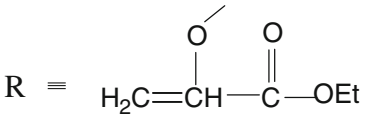

We expect that microwave irradiation lead to a scission of the bond as close to Ti atom as possible in the complex. This leads to two possibilities as shown below:

Mechanism 1:
$$[TiOR_2]_2 \rightarrow 2TiO^{2+} + 4R^-$$
$$2TiO^{2+} + 2H_2O \rightarrow 2TiO_2 + 4H^+$$
$$4R^- + 4H^+ \rightarrow 4RH$$

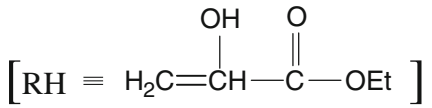

(RH simply escapes or is further degraded in the microwave oven).

Mechanism 2:
$$[TiOR_2]_2 \rightarrow 2Ti^{4+} + 2R_2O^{4-}$$
$$2R_2O^{4-} + 4H_2O \rightarrow 4RH + 4O^{2-}$$
$$2Ti^{4+} + 4O^{2-} \rightarrow 2TiO_2$$

In both mechanisms, reactions eventually re-form the organic part (the β-keto ester) while water, essential for the reactions, is not added at the beginning. It is entirely possible that R^- and R_2O^{4-} decompose under irradiation in a subsequent stage, and give rise to H_2O as one of the products, so that the reaction does not require addition of water. But we note that the addition of a few drops of water into the reaction vessel increases yield of the oxide remarkably. This phenomenon clearly supports the view that the reaction proceeds via use of H_2O which may be a byproduct of microwave reaction. However, the two mechanisms cannot be distinguished easily without labeling oxygen atoms in either the precursor or the H_2O, and then examining the oxide for the presence of the labeled oxygen atom. If the reaction proceeds

Table 1. Summary of grain size and phases formed from calcinations of microwave derived TiO_2 at different temperatures.

Temperature of calcinations (°C)	Main phase of TiO_2 identified by XRD	Other phase of TiO_2 identified by XRD	Grain size calculated from Scherrer equation using high intense peak (nm)
150	Amorphous	-	-
400	Anatase	-	17
500	Anatase	Rutile	26
600	Anatase + rutile	-	26
700	Rutile	Anatase	35
800	Rutile	-	40

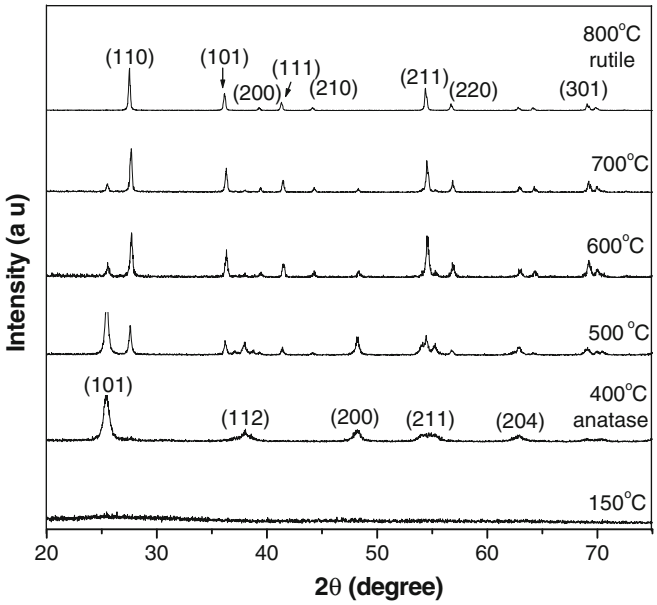

Figure 1. X-ray diffraction patterns of TiO_2 samples calcined at different temperatures for 6 h.

via mechanism 2, product TiO_2 would not contain the labeled oxygen if the precursor had labeled oxygen; if it proceeds by mechanism 1, it would. With the use of oxygen-labeled water, we would expect the product TiO_2 from mechanism 2 to contain twice the amount of labeled oxygen than when TiO_2 is formed by mechanism 1. At this time, we have not performed these studies. The precursor molecule used was devoid of water of crystallization and the formation of oxide was dependant exclusively on the water available either from the atmosphere or from the microwave reaction itself via a mode of break down of R (or even PVP) which is as yet unclear. Nevertheless, without water addition, yields of TiO_2 were observed to be very low.

XRD patterns of titania powders dried at room temperature and calcined at different temperatures for 6 h are shown in figure 1. The as-prepared TiO_2 powder, even after calcining at 150°C, was found to be amorphous. The powder crystallized when it was heated at 400°C for 6 h, and XRD pattern indexed excellently to that of TiO_2 in the anatase form. The average size of crystallites was calculated from the half-width of the peak using the Scherrer equation (Cullity 1978). The estimated mean size of the anatase particles sintered at 400°C was 17 nm, by attributing the broadening solely to particle size effect. Only one phase, anatase, exists below 500°C. Phase transformation from anatase to rutile is found to occur at 500°C and above. The calcination is usually accompanied with crystal growth (Edelson and Glaeser 1988). XRD pattern of TiO_2 heated at 500°C reveals the anatase (101) reflection associated with an emerging rutile (110) reflection. The sample calcined at 500°C is indeed a mixture of both anatase and rutile phases. Calcination at 600°C and above resulted in a change in the intensities of the peaks. The rutile peak increased while anatase peak decreased in intensity with increase in calcination temperature. The calculated nanoparticle sizes and phases formed at different temperatures are given in table 1. Evolution of rutile peak during isothermal annealing of the material at 600°C is shown in figure 6. Percentage of rutile formed as a function of time is listed in table 2 which shows that $A \rightarrow R$ transformation occurs with significant isothermal kinetics. In view of additional data being collected kinetic aspects are not discussed any further in this paper.

Table 2. Percentage of rutile phase in TiO_2 samples as a function of time at 600°C.

Calcination time (h)	Percentage of rutile phase
2	44
4	57
8	65
16	70
24	77
48	86

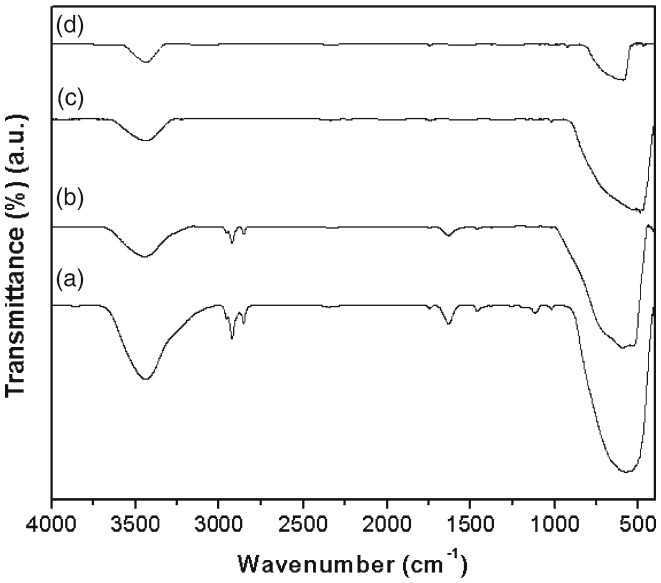

Figure 2. FT–IR spectra of nanophase TiO_2 samples calcined at different temperatures for 6 h.

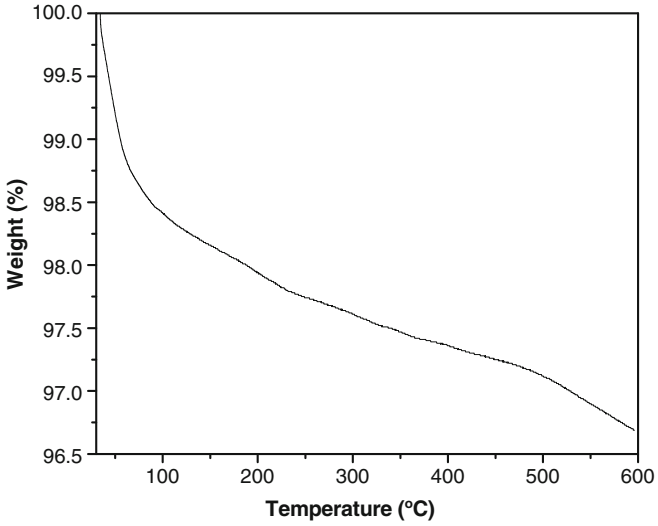

Figure 4. TGA pattern of as-synthesized TiO_2 sample.

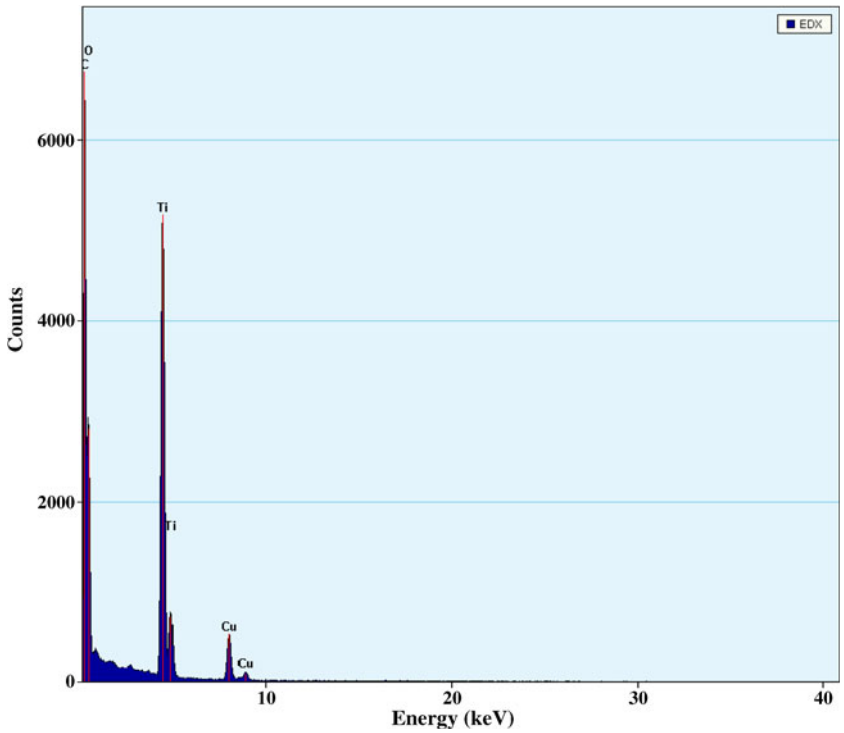

Figure 3. EDX pattern of TiO_2 nanoparticles.

FT–IR spectra of nanophase TiO_2 calcined at different temperatures for 6 h are shown in figure 2. The TiO_2 samples show a broad band centred around 3440 cm^{-1}, which is due to H-bonded OH groups arising from adsorbed water. Indeed, a band at 1631 cm^{-1} due to water deformation modes was also observed. The three bands in the C–H stretching region at 2960 cm^{-1}, 2927 cm^{-1}, and 2850 cm^{-1} can be attributed to adsorbed PVP on the surface of TiO_2 calcined at lower temperatures. The C–H bending vibration was observed as a small band at 1461 cm^{-1}. The disappearance of the peaks corresponding to C–H stretching and bending vibrations at higher temperatures can be ascribed to desorption and decomposition of PVP. The number of hydroxyl groups on the surface of TiO_2 is proportional to the intensity of the peak at 3440 cm^{-1}. Even after calcination at 800°C, TiO_2 exhibited only a decrease in the intensity

of the 3440 cm^{-1} band. This is an indication that some water molecules are tightly bound to the rutile surface. The broad band observed at 560 cm^{-1} can be attributed to Ti–O stretching vibration, and it shifts to lower wavenumbers with increase in temperature.

Figure 3 shows EDX pattern of TiO_2 nanoparticles. No impurity elements could be detected within the detection limits. Copper and carbon peaks arise from coated copper grids used in our studies. The absence of any impurities is critical for the anatase rutile transformation to be discussed later.

Figure 4 shows the plot obtained from thermogravimetric analysis of as-synthesized TiO_2 in nitrogen. There are three apparent stages of decrease in specimen weight. The first one occurs over a temperature range 25–170°C, the second one occurs over a temperature range 170–500°C, and the third one from 500–600°C. The first loss of weight can be attributed to the release of adsorbed water, and the second to desorption and decomposition of the surfactant material. We attribute the third to the decomposition of residual organics (R or PVP) and fragments bound to TiO_2 nanoparticle surface. However, the origin of this enthalpic region is unclear to us at this stage. We may infer with confidence that the surfactant PVP in the as-synthesized TiO_2 is essentially completely eliminated around ∼500°C.

Figures 5(a) and (b) are SEM and TEM micrographs of TiO_2 calcined at 500°C for 6 h. From figure 5(a), it is apparent that the resulting TiO_2 is a compact arrangement of uniformly sized nanoparticles. Regular and well-crystallized nanoparticles of TiO_2 can be seen in figure 5(b). The TEM micrograph suggests that the particles have not really agglomerated. The average size of particles is estimated from TEM to be ∼25 nm and is consistent with the value calculated from the peak broadening in XRD of heated samples. TiO_2 exhibits a relatively narrow particle size distribution, with ∼90% of the particles in the size range of 20–30 nm. It seems that the surfactant provides extraordinary control on the sizes of nanoparticles, and also prevents extensive growth of the particles particularly in the rutile phase. The electron diffraction pattern corresponding to figure 5(b) is shown in figure 5(c).

3.1 *Anatase–rutile phase transformation*

TiO_2 is known to exhibit rich phase formation behaviour. It manifests at least seven crystal structures, besides the famous infinitely-adaptive structures of non-stoichiometric TiO_{2-x}. Anatase, brookite and rutile phases are among the most investigated (Rao and Rao 1978). While rutile is the more stable form of TiO_2 at room temperature and pressure for large crystallite sizes, anatase seems to become stable when particle size is very low. Nanocrystalline TiO_2 with crystallite size <14 nm have been shown to possess the anatase structure (Gribb and Banfield 1997). Evidently, surface energies seem to influence phase stability (Zhang and Banfield 1998). Thermochemical measurements reported from

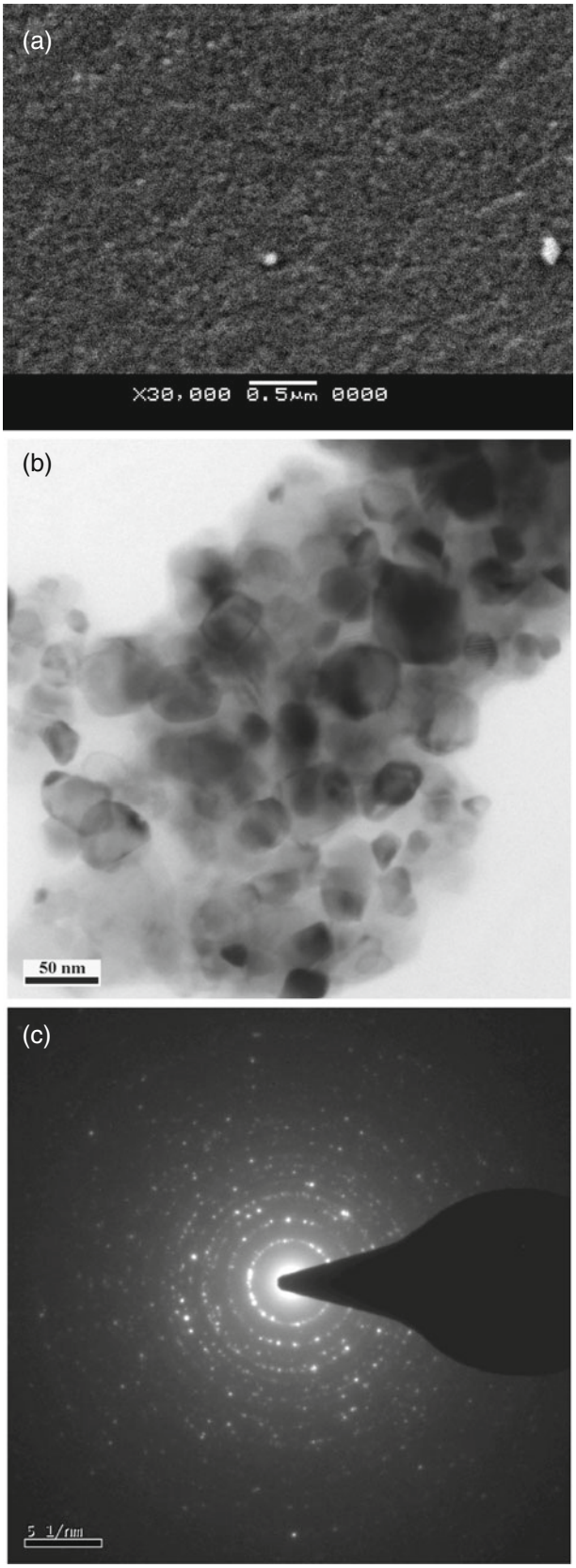

Figure 5. (**a**) Scanning electron micrograph, (**b**) transmission electron micrograph and (**c**) corresponding electron diffraction pattern of TiO_2 nanoparticles calcined at 500°C for 6 h.

Navrotsky's laboratory (Ranade *et al* 2002) show that surface energy of anatase (0·4 J/ m^2) is less than a fifth of the surface energy of the rutile phase (2·2 J/m^2), which more than compensates for the ∼2·6 kJ/mol higher enthalpic stability of rutile over anatase when particle sizes are ∼14 nm. Although the brookite phase has intermediate enthalpy values and is expected to result from the transformation of anatase, it appears that very small particles, such as those formed in sol–gel processes, often give rise to a mixture of anatase and brookite, and both transform to rutile. The possibility that anatase transforms into brookite and then to rutile has also been discussed by Zhang and Banfield (2000). However, it was observed by Ye *et al* (1997) that brookite may transform into anatase and then to rutile. In their extensive and insightful investigations of phase transition of TiO_2, Lee Penn and Banfield (1998) observed that brookite is a polytype of anatase and its inter-conversion only involves the displacement of titanium atoms into adjacent octahedral sites. In somewhat related work on the preparation of mesoporus titania, Correa and co-workers (dos Santos *et al* 2009) have shown that creation of defects by sonication can bring about anatase–to–rutile transformation at lower temperatures. Banfield and Veblen (1992) have proposed a very attractive transformation mechanism based on a structural concept of 'fundamental building blocks'. They have suggested that a block of anatase could, by the simple operation of a shear, transform to rutile structure.

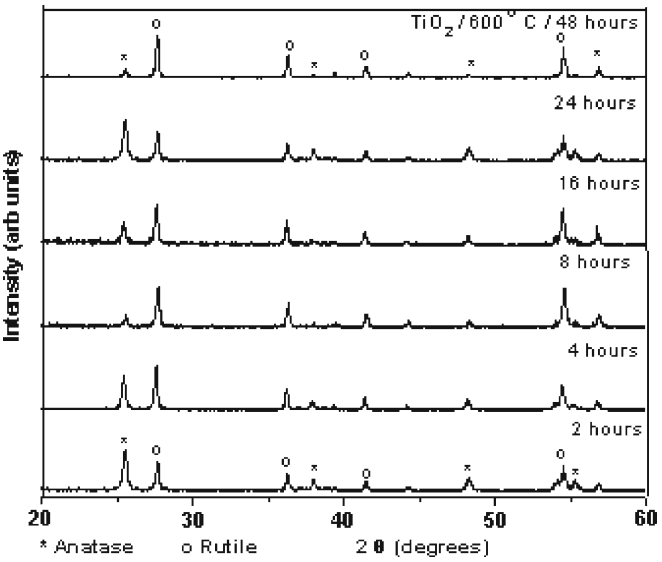

Figure 6. XRD patterns of titania samples obtained by calcination at 600°C for 2 h, 4 h, 8 h, 16 h, 24 h and 48 h, respectively.

In view of the various anatase-to-rutile transformation mechanisms discussed in the literature and the findings in this paper, this basically irreversible transformation merits a brief relook. We first note that (i) the transformation is actually from anatase (A) to rutile (R) rather than A to brookite (B) to R, and that the particle sizes are indeed very small in the present case, (ii) we have not found any evidence in XRD for the $A \rightarrow B$ transformation (figure 1), which is consistent with the observation made by Lee Penn and Banfield that B is only a polytype of A. Even if there is an $A \rightarrow B \rightarrow R$ transformation, B is likely to be rather metastable, and appear only as a transitory phase, (iii) the transformation $A \rightarrow R$ occurs only at sufficiently high temperatures with a considerably high activation barrier (∼100 kcal/mol) (Czanderna *et al* 1958; Rao 1961; Shannon and Park 1965; Zhang and Banfield 1999; Hsiang and Lin 2008), (iv) there

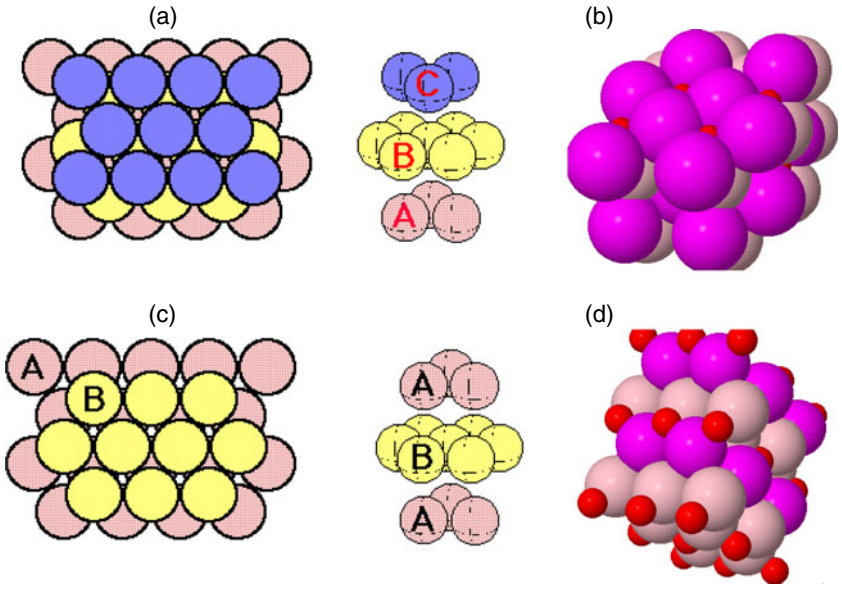

Figure 7. (**a**) Ideal cubic close packing, (**b**) packing of O^{2-} ions in anatase (Ti^{4+} ions in red), (**c**) ideal hexagonal packing and (**d**) packing of O^{2-} ions in rutile (from www.firstyear.chem.usyd.edu.au and www.seas.upenn.edu).

seems to be experimental evidence that the $A \rightarrow R$ transformation is characterized by the orientation relationship $\{101\}_A$ // $\{101\}_R$ and $<201>_A$ // $<111>_R$ (Shao *et al* 2004) and (v) lattice shear appears to accomplish the $A \rightarrow R$ transition (Lee Penn and Banfield 1998), although it is not a martensitic type of transition (Rao and Rao 1978). Ti^{+4} in TiO_2 is highly ionic and in bulk of both *A* and *R* phases, always octahedrally coordinated to O^{2-} (Woning and Van Santen 1983), O^{2-} ions are present in an approximately close packed but slightly distorted lattice arrangement, as noted very early by Simons and Dachille (1970). Ti^{+4} ions occupy quarter of the octahedral holes of the possible two close packing motifs, viz. *ccp* and *hcp* (figure 7). O^{2-} ions are in distorted *ccp* packing geometry in anatase and in distorted *hcp* packing in rutile (Hyde *et al* 1974; Banfield and Veblen 1992).

Thus, the $A \rightarrow R$ transformation, viewed from the O^{2-} ion sublattice, is a change from the ABCABC (distorted) packing geometry to the ABABAB (distorted) packing geometry. This can be accomplished in two ways: (I) In a block of 6 layers *ABCABC*, the *AB* block is preserved and every layer in the remaining *CABC* block is rotated as a whole to make it *ABAB* ($C \rightarrow A$; $A \rightarrow B$; $B \rightarrow A$; $C \rightarrow B$). In fact, when *C* changes to *A*, it finds the next layer to be *A*, which makes for intrinsic instability, and rotates as a whole either to *B* or *C*. Change to *B* accomplishes the required transformation. The last change would be to rotate the *C* layer into the *A* layer position. These operations are understandably fairly energetic, shape-preserving 'shear' operations, as can be appreciated by working with models, and (II) the transformation can also be achieved by the following imaginary operation in which every third layer (*C* layer) is pulled out and placed at the surface as an extended lattice layer. The new layer can be stacked as *ABAB* etc. Energetically, this placement first involves the creation of two new surfaces around the layer which is pulled out, and this energy is fully recovered when the layer which is pulled out is placed such that it extends the lattice. The collapse of the *ABAB* layer converts anatase blocks to rutile blocks, releasing a net energy corresponding to the enthalpy of the $A \rightarrow R$ phase transformation. The activation barrier in this virtual process is the energy required to pull out a single oxygen layer, along with Ti^{4+} ions belonging to that layer (neutral $Ti_{1/2}O$ layer). This operation of pulling out the thinnest 2-*d* slice of the lattice requires rather significant energy.

But the activation energy required to rotate the layer in such a way that *C* changes to *A* etc is just the energy needed to cause a virtual disentanglement of the $[Ti_{1/2}O]$ layer from the rest of the TiO_2 structure and to provide for the restricted movement of this layer, without losing the cohesion in the layer itself. We may note here that Simons and Dachille had very early noted that a shear of O^{2-} ion layers can indeed be considered as a mechanism of transformation. This is in essence a 'layer excitation' induced transformation. The cohesion in the layer is largely due to columbic interactions of the O^{2-} and Ti^{+4} ions (the repulsive O^{2-}– O^{2-} and Ti^{4+}–Ti^{4+} interactions contribute typically ∼10% of the attractive columbic energy). A reasonable estimate of this energy is equal to the cohesive energy of the $Ti_{1/2}O$ layer itself. When the energy corresponding to the difference in cohesive energies of the bulk and the layer is supplied to the system, the $Ti_{1/2}O$ layer is isolated and it can begin to rotate or reorganize cooperatively, so that it nucleates the transformed rutile phase. With this assumption, we may identify the associated activation energy with the additional energy required to decrease the cohesion and create an isolated layer. This is indeed the cohesive energy of $2D$ TiO_2. It is nontrivial to evaluate the energy of a mol of planar TiO_2 (2-*D* TiO_2). Intuitively, cohesive energy must be a strong function of the dimensionality, *D*, particularly when the bonding is predominantly ionic.

The cohesive energy of the layers has indeed been examined long ago by Woning and Van Santen (1983) while considering surface reducibilities of rutile and anatase. For purposes of providing a semi-quantitative explanation we approach the problems as follows. When NaCl (*Fm*3*m*) is sliced and spread out to a two-dimensional lattice the effective Madelung constant decreases from 1·7475 of the 3D crystal to 1·6165 of the 2D crystal. It goes down further to 1·3862 for the 1D NaCl crystal. Assuming that, to a first approximation nearest interionic distances do not vary much the cohesive energies of the $2D$ at $1D$ forms of NaCl scale as the corresponding Madelung constants. Variation of the Madelung constants as a function of dimensionality for the case of NaCl can be expressed as

$$M(D) = M_0 D^n,$$

(see figure 8 for the logarithmic plot), where $M_0 = 1{\cdot}3874$ and $n = 0{\cdot}2125$; *n* is the exponent of dimensionality. It may be noted that $M(1) = M_0$ because $D = 1$. We may consider that Madelung constants of $2D$ and $1D$ anatase and rutile also possess the same functional form although not the

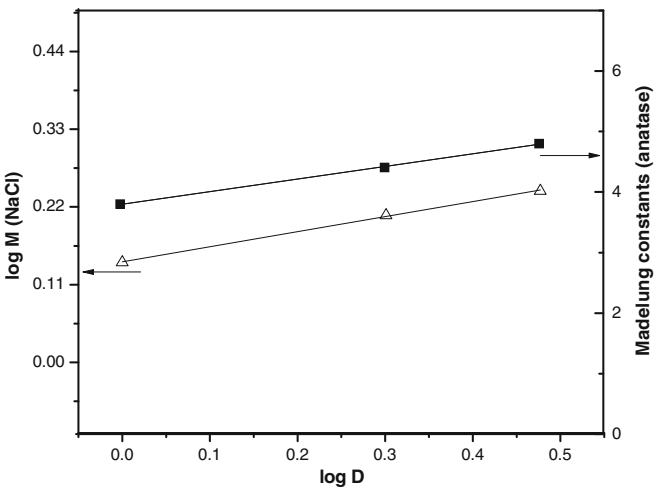

Figure 8. Logarithmic plot of Madelung constants vs dimensionality. In case of NaCl, Madelung constants are known. In case of anatase it has been plotted assuming exponent as 0·2125.

same values of the constants, M_0 and n. In the absence of reported values of Madelung constants for the $2D$ and $1D$ anatase or rutile structures, we assume that n has the same value of 0·2125 for anatase and calculate the corresponding M_0, M_0 turns out to be 3·8134. On the basis of this M_0 value, $M(2)$ of the $2D$ anatase is found to be equal to 4·4026. It is interesting to note that this is marginally lower than the Madelung constant of (001) surface layer (= 4·4505) calculated by Woning and Van Santen (1983). Further since lattice energies scale with the Madelung constant, $2D$ anatase can be expected to have a lattice energy of (4·4026/4·800) × 13699 kJ/mol = 12565 kJ/mol. Thus the additional energy to be provided to $3D$ anatase to make it $2D$ anatase is equal to (13699–12565) kJ/mol = 1134 kJ/mol = 271 kcal/mol. This energy is more than twice the observed activation energy of $A \rightarrow R$ transformation. The reason may not be far to find.

It is unphysical to expect a total isolation of an intermediate TiO_2 layer in order to enable it to undergo rotation or reorganization in order to nucleate transformation. Even as the layer is separated by short distance from the rest of the crystal, the transformation to rutile can begin to occur. Thus if the layer Madelung constant decreases to only 4·6 the energy needed would be only about half or about 130 kcal/mol. That is even as the layer gets to be slightly separated from the neighbouring regions in anatase and the Madelung constant begins to drop from its $3D$ value of 4·80 to about 4·60; and the process of $A \rightarrow R$ conversion can begin without having to have the $M(3)$ drop to $M(2)$. Since we identify this as the activation energy for the $A \rightarrow R$ transformation it is seen that it is in reasonable agreement with the experimentally observed values mentioned above (∼100 kcal/mol). In actual process, the layer is not expected to get distanced from the rest of the crystal as in this virtual process, but the required energy is made available at the high temperature of transformation in the form of activation energy. Therefore, it appears that anatase → rutile transformation may involve a mechanism in which enough energy is provided to a TiO_2 ($2Ti_{1/2}O$) layer to facilitate a rotation of the plane or reorganization of ions. We feel that nanocrystallites take full advantage of such 'layer excitations' because of their small size. The shear modulus of anatase is 90 GPa and its density is 3·84 g/cc. The shear sound velocity can be calculated as $\sqrt{g/\rho} \approx 4{\cdot}8 \times 10^7$ cm/s. Assuming that the shear wavelength is ∼30 nm, and that it corresponds to one exciting shear wavelength, the corresponding shear wave frequency is found to be $1{\cdot}6 \times 10^{13}$/s. The corresponding shear phonon energy is 1·3 kcal per mol. This may be compared to the thermal energy of ∼ 650 × 2 cal/mol. Therefore, the probability of such excitations is ∼1/e or is very high. Hence we believe that the layer excitations are readily accomplished. We also feel that layer rotation is more likely than layer reorganization. The preservation of some of the lattice planes through the transformation as observed in earlier studies is a likely consequence of the operation of this mechanism.

Such a mechanism also supports other observations associated with the $A \rightarrow R$ transformation. From very early times, the Avrami kinetic model has provided insights into the $A \rightarrow R$ transition. The induction time observed in bulk samples of pure anatase is essentially absent in the transformation of nanoparticles. As mentioned above the nanoparticles by virtue of their extremely small size easily support layer excitations. The transformed rutile phase is denser (4·27 g/cc) while untransformed anatase is of low (3·90 g/cc) density. Thus $A \rightarrow R$ transformation suffers no transformation inhibition from the matrix. Indeed, the nucleation of rutile may become facile and the growth stage faster. Transformation of ionic layers which undergo excitation could be assisted by the presence of aliovalent impurities which give rise to oxygen vacancies but tend to retain layer integrity. This is evidenced in many reported studies (dos Santos *et al* 2009). This aspect has not been examined fully in the $A \rightarrow R$ transformation of nano-TiO_2. However, impurities like SO_4^{2-}, PO_4^{3-} can inhibit phase transformation by inhibiting O^{2-} layer separation (SO_4^{2-}, PO_4^{3-}). This aspect is well established in the bulk (Bursill and Hyde 1972), but has not been examined in nano-TiO_2. We expect the impurity effects to be more pronounced in nanometric samples.

In the bulk, the phase transformation in TiO_2 was first noted as a second order transformation by Czanderna *et al* (1958) and it was reexamined by Rao (1961) using pure anatase who found it to be a first order transformation. In the present model, the rate of creation of activated or excited layers can increase very steeply when the transformation temperature is exceeded even marginally. Coupled with the exothermicity of the transformation, the phase transition should be expected to be first order, as noted long ago by Rao (1961). Since nanometric anatase particles possess a high surface–to–volume ratio, the activation barrier which we identify as energy required for layer excitation exhibits a significant spread in values rather than being distinct for the 'in surface' and 'in bulk' layers. This spread is likely to manifest in the phase transformation appearing to be smeared and of the second-order at the beginning and changing over rapidly and dominantly to a first order transformation. We do not favour the likelihood of transformation occurring first at the surface of nanoparticle, $A \rightarrow$ disordered surface layer, surface R phase → propagation of transformation inwards for two reasons. One, the transformed R phase cannot exploit the volume shrinkage to induce neighbouring layers to respond readily. Second, the enthalpy of transformation is given away to other particles or to the environment if it were a surface initiated transformation rather than being confined to inter layer region and increase the local temperature for more efficient transformation.

4. Conclusions

Preparation of nanocrystalline titania has been achieved by a microwave irradiation-assisted process using the precursor $[TiO(etob)_2]_2$ and PVP. In contrast to other methods of synthesis, microwave irradiation has the advantage of uniform,

rapid, and volumetric heating. Nanocrystalline TiO_2 with varying amounts of anatase and rutile phases was obtained by careful control of the calcination temperature of the anatase powder resulting from the microwave-assisted process. The nanosized TiO_2 obtained by this method is a potential candidate as a photocatalyst for air and water purification. Many curious features of the $A \rightarrow R$ transition of TiO_2 in nanoparticles are discussed, and it is suggested that the transformation occurs through a mechanism of layer excitation leading to the needed rotation or reorganization which nucleated the transformed *R*-phase in the distorted cubic close packed O^{2-} ion structure of the anatase phase. The microwave process has proved to be an effective alternative to conventional techniques for the fast synthesis of homogeneous titanium dioxide.

References

Baldassari S, Komarneni S, Mariani E and Villa C 2005 *J. Am. Ceram. Soc.* **88** 3238

Banfield J F and Veblen D R 1992 *Am. Mineral.* **77** 545

Bursill L A and Hyde B G 1972 *Nature Physical Sci.* **240** 122

Cozzoli P D, Kornowski A and Weller H 2003 *J. Am. Chem. Soc.* **125** 14548

Cullity B D 1978 *Elements of X-ray calcination* (Reading, MA: Addison-Wesley)

Czanderna A W, Rao C N R and Honig J M 1958 *Trans. Faraday Soc.* **54** 1069

dos Santos J G, Ogasawara T and Correa R A 2009 *Brazilian J. Chem. Calc.* **26** 555

Edelson L H and Glaeser A M 1988 *J. Am. Ceram. Soc.* **71** 225

Gribb A A and Banfield J F 1997 *Am. Mineral.* **82** 717

Hsiang Hsing-I and Lin Shih-Chung 2008 *Ceram. Int.* **34** 557

Hyde B G, Bagshaw A N, O'Keefe M and Andersson S 1974 *Ann. Rev. Mater. Sci.* **4** 43

Jang S, Vittal R, Lee J, Jeong N and Kim K 2006 *Chem. Commun.* **1** 103

Jansen J C, Arafat A, Barakat A K, Van Bekkum H, Occelli M L and Robson H 1992 *Synthesis of microporous materials* (New York: Van Nostrand Reinhold)

Karch J, Birringer R and Gleiter H 1987 *Nature* **330** 556

Kominami H, Muratami S, Kato J, Kera Y and Ohtani B 2002 *J. Phys. Chem.* **B106** 10501

Kumar S, Panneerselvam M, Vinatier P and Rao K J 2004 *Ferroelectrics* **306** 165

Lee Penn R and Banfield J F 1998 *Am. Mineral.* **83** 1077

Matsunaga T and Inagaki M 2006 *Appl. Catal. B: Environ.* **64** 9

Murugan A V, Samuel V and Ravi V 2006 *Mater. Lett.* **60** 479

Nakade S, Matsuda M, Kambe S, Saito Y, Kitamura T, Sakata T, Wada Y, Mori H and Yanagida S 2002 *J. Phys. Chem.* **B106** 10004

Ohshima T, Nakashima S, Ueda T, Kawasaki H, Suda Y and Ebihara K 2006 *Thin Solid Films* **506** 106

Panda A B, Glaspell G and El-Shall M S 2006 *J. Am. Chem. Soc.* **128** 2790

Panneerselvam M and Rao K J 2003a *J. Mater. Chem.* **13** 596

Panneerselvam M and Rao K J 2003b *Chem. Mater.* **15** 2247

Parking I P and Palgrave R G 2005 *J. Mater. Chem.* **15** 1689

PEW 2009 *Projects on Emerging Nanotechnologies*

Ranade M R *et al* 2002 *PNAS* **99** 6476

Rao C N R 1961 *Can. J. Chem.* **39** 498

Rao C N R and Rao K J 1978 *Phase transitions in solids* (New York: McGraw Hill)

Shalini K, Chandrasekaran S and Shivashankar S A 2005 *J. Cryst. Growth* **284** 388

Shannon R D and Park J A 1965 *J. Am. Ceram. Soc.* **48** 391

Shao Y, Tang D, Sun J, Lee Y and Xiong W 2004 *China Particuology* **2** 119

Simons P Y and Dachille F 1970 *Am. Mineral.* **55** 403

Tang J, Redl F, Zhu Y, Siegrist T, Brus L E and Steigerwald M L 2005 *Nano Lett.* **5** 543

Wei M, Konishi Y, Zhou H, Yanagida M, Sugihara H and Arakawa H 2006 *J. Mater. Chem.* **16** 1287

Woning J and Van Santen R A 1983 *Chem. Phys. Lett.* **101** 541

Ye X S, Sha J, Jiao Z K and Zhang L D 1997 *Nanostruct. Mater.* **8** 919

Zhang H and Banfield J F 1998 *J. Mater. Chem.* **8** 2073

Zhang H and Banfield J F 1999 *Am. Mineral.* **84** 528

Zhang H and Banfield J F 2000 *J. Phys. Chem.* **B104** 3481

Zhu Y, Shi J, Zhang Z, Zhang C and Zhang X 2002 *Anal. Chem.* **74** 120